Repositioning of Parabolic Antenna Panels Onto a Shaped Surface

R. Levy
DSIF Engineering Section

Optimal parameters for shifting existing parabolic reflector surface panels for re-use within shaped antenna configurations are determined from theory and equations given in this article. The panels are reset to minimize the rms half-pathlength differences between their surface and the ideal, shaped surface. Input, output, and results are described for a computer program that implements the equations. Results for typical 26- and 64-m antennas indicate that, if all or most of the existing parabolic panels are re-used and repositioned according to the procedure, the consequent rms differences will be small.

I. Introduction

Gain enhancement for existing parabolic antenna reflectors has been discussed by Ludwig (Ref. 1) and Potter[1]. One improvement is to modify the hyperbolic subreflector and parabolic main reflector surfaces with slightly different, "shaped" surfaces, which can provide nearly uniform aperture illumination. To do this, completely new subreflectors are anticipated, because the usual subreflector structural configurations are not readily adaptable to surface and envelope changes. However, the main reflector surface typically is formed from many individual panels that can be repositioned to provide a good approximation to the new shaped surface. The approximation depends, of course, upon how closely the original parabolic surface within each panel approaches the shaped contour. These errors tend to be small near the center of the antenna and increase towards the rim.

This article presents the geometrical and mathematical relationships used in a computer program that generates optimal new coordinates for repositioning parabolic panels for a shaped surface reflector. These coordinates are selected to minimize differences of the RF energy beam from the path that would be provided by the ideal shaped surface.

II. Approach

Figure 1a shows a radial section of a typical antenna. The solid curve represents the original parabolic surface, and the broken curve represents the desired new shaped

[1]"Antenna Study: Performance Enhancement" by P. D. Potter in this issue.

surface. The actual distances between the two curves are exaggerated for clarity. As an example, for the 64-m antenna at the Mars DSS (DSS 14), the maximum distance in the focal direction is only about 2 cm.

Figure 1b shows a typical panel that has been shifted towards the shaped surface. The shifted panel maintains the original curvature, but, because of the inner and outer edge translations, distances from the shaped surface are significantly reduced.

The procedure that will be given here is used to define new edge translations that minimize the weighted rms pathlength deviations from the shaped surface for a discrete set of points distributed over each panel. Since the objective of surface shaping is to provide uniform aperture illumination, the weighting factors are the aperture areas tributary to each of the points. The set of points used in the procedure is the set defined for the shaped surface generated by the computer program Dual Reflector Antenna System Design (DAR) (Ref. 2). This program generates focal-axis shaped coordinates and the angle at the surface between incident and emergent rays for a closely spaced discrete set of points spaced, for example, on an average of about 15 cm in the radial direction for the 64-m antenna.

All relationships developed are based upon a linearization of the actual geometry. In this, the surface between two points closely spaced in the radial direction is approximated by the tangent to the surface at either point. This is reasonable because curvatures are relatively flat and do not have rapid local changes. Furthermore, in developing the parameters for shifting the parabolic panels, it is noted that the shifts are of differential magnitude with respect to the overall geometry, and that the sines and cosines of associated angles of rotation can be replaced by the angle and by unity, respectively. It can be confirmed by calculation that the related approximations in these linearizations are of higher order than the pathlength deviations and shift dimensions.

III. Pathlength Difference Geometry

Figure 2 shows a typical incident ray at radius r that would be reflected towards the subreflector at the angle β after impinging on the shaped surface at point a. Points b and c are, respectively, points on a parabolic panel at the same radius before and after shifting the panel. Points d and e are auxiliary points used to define distances associated with pathlength differences. Expressions will be given for the difference in the path of a ray reflected by a parabolic panel with respect to the path of a ray reflected by a point on the shaped surface.

Before shifting the panel, the initial difference in pathlength is

$$\underline{DP} = \overline{ad} + \overline{ae} \tag{1}$$

To evaluate $\underline{DP}$ in terms of the parameters of the shaped and parabolic surfaces, let the parabolic curve, with focal length f, be defined in terms of the focal-axis coordinate z and the radial coordinate r as

$$z - r^2/4f = 0 \tag{2}$$

and let the slope be defined as

$$ZP = \frac{dz}{dr} = r/2f \tag{3}$$

Let $DZ = \overline{ab}$ = original difference in the z coordinate between the panel and shaped surfaces. Then, from Fig. 2,

$$\overline{bd} = \overline{de} \cdot ZP \tag{4}$$

$$\overline{de} = \overline{ad} \cdot \tan\beta \tag{5}$$

$$\begin{aligned}\overline{ad} &= DZ - \overline{bd} \\ &= DZ - \overline{ad} \cdot ZP \cdot \tan\beta\end{aligned} \tag{6}$$

Solving Eq. (5) for $\overline{ad}$,

$$\overline{ad} = DZ/(1 + ZP \cdot \tan\beta) \tag{7}$$

Also,

$$\overline{ae} = \overline{ad}\sec\beta \tag{8}$$

Therefore, substituting Eqs. (7) and (8) in Eq. (1),

$$\underline{DP} = DZ \cdot S \tag{9}$$

where

$$S = (1 + \sec\beta)/(1 + ZP \cdot \tan\beta) \tag{10}$$

After shifting the panel through an amount $DELZ$ at radius r, the difference in the z coordinate from the panel to the shaped surface is $DZ + DELZ$. Therefore, by analogy with Eq. (9), the pathlength difference, DP, for the shifted panel is

$$DP = (DZ + DELZ) \cdot S \tag{11}$$

Except for *DELZ*, all terms in Eq. (11) are obtained from either the original parabolic geometry or the output of the DAR program. In the following, *DELZ* will be expressed in terms of two shift parameters for each panel: a rigid body z direction shift, H, and a rotation angle, ϕ. The shift parameters are then chosen to minimize the sums of the weighted pathlength deviations for the set of points for which new shaped coordinates are supplied by the DAR program.

IV. Computation of Weighting Factors

The weighting factor based upon the aperture area tributary to the pth radius within the kth panel will be derived with reference to Fig. 3. According to the figure, let R_A and R_B be the inner and outer boundary radii, respectively, for this panel, and let n be the number of radii for which shaped surface coordinates are defined; assume temporarily that all of the panels (with various boundary radii) have a common central sector angle θ.

Then, an appropriate weighting factor, W_p, for a typical interior radius, r_p, of this panel is

$$W_p = [(r_p + r_{p+1})^2 - (r_p + r_{p-1})^2]/4 \tag{12}$$

The weighting factor for the first point in this panel (at radius r_1) is

$$W_1 = [(r_1 + r_2)^2 - 4R_A^2]/4 \tag{13}$$

The weighting factor for the last point in this panel (at radius r_n) is

$$W_n = [4R_B^2 - (r_n + r_{n-1})^2]/4 \tag{14}$$

The weighting factors are normalized so that the sum of these factors at all radii is equal to the number of DAR points for the entire aperture. The corresponding normalization factor F is

$$F = NT/(R_{\max}^2 - R_{\min}^2) \tag{15}$$

where

$$NT = \sum_{k=1}^{m} n_k \tag{16}$$

in which m is the number of panel rings; n_k is the number of radii in the kth panel; and $R_{\max}$ and $R_{\min}$ are, respectively, the maximum and minimum radii for the aperture.

The pathlength differences are computed within an antenna aperture sector defined by the central angle θ, which is taken as the central angle for the innermost panel. At each panel, this sector can be further subdivided for pathlength computations into J sections in the circumferential direction. Then, letting J_k = number of circumferential sections for the kth panel, a second set of weighting factors equal to $1/J_k$ is defined for each panel, and the weighting factor previously derived for the pth radius within the panel is multiplied by $1/J_k$ for the J_k points that are considered at this radius.

V. Computation of Pathlength Difference for Panel Shift Parameters

This computation requires that the focal-axis coordinate change term, *DELZ* according to Eq. (11), which is the sum of a panel rigid body shift, H, plus components caused by the rotation, ϕ. The rotation components can be derived in terms of ϕ from the original parabolic geometry shown in Fig. 4. In Fig. 4a, a typical parabolic panel, which subtends central angle TR, is shown projected on a plane parallel to and above the aperture plane. The panel projection consists of the radial lines, $\overline{bd}$ and $\overline{ce}$, and the chords, $\overline{bc}$ and $\overline{de}$. In Fig. 4b, the height, Z_A, of the projection plane above the aperture plane is

$$Z_A = [RA \cdot \cos(TR/2)]^2/4f \tag{17}$$

A local coordinate system is defined by the V axis, to give the distance above the projection plane, and the X axis, which is taken along the panel centerline and represents the distance measured outward from a plane parallel to the Z axis and containing $\overline{bc}$. The axis of rotation is parallel to $\overline{bc}$ and intersects the origin of the local coordinate system. Rotations are measured positive counterclockwise, as shown. Point p, with coordinates V_p and X_p, is on the parabolic panel before rotation and is located at radius R_p with respect to the focal axis, and at angle TS_c from the panel centerline. For J_k = the number of central angle subdivisions for this panel, TS_c is determined from

$$TS_c = C \cdot TR/J_k, \qquad C = 1/2, 3/2, \cdots, (J_k - 1)/2 \tag{18}$$

Rotation has two effects on *DELZ*. The first is to bring p', originally at radius $R_p + \Delta R_p$, inwards by ΔX_p and directly over p. The second is the change in the V coordinate due to rotation, which is approximately the same for p and p'. The rotation component of *DELZ*, which is the distance pp'', is the sum of these two effects. This sum is approximately

$$DELZ = \Delta R_p \cdot ZP + \phi \cdot (X_p + \Delta X_p) \tag{19}$$

However,

$$\Delta R_p \simeq \Delta X_p \cdot \cos TS_c \tag{20}$$

$$\Delta X_p \simeq \phi\,(V_p + \Delta R_p \cdot ZP) \tag{21}$$

Substituting Eqs. (20) and (21) in Eq. (19) and neglecting quadratic and higher-order terms in ϕ and ΔX_p leads to the rotation component:

$$DELZ = \phi \cdot (V_p \cdot \cos TS_c \cdot ZP + X_p) \tag{22}$$

Adding the rigid body shift H, the total focal-axis shift at the original point p becomes

$$DELZ = H + \phi \cdot T_c \tag{23}$$

where

$$T_c = V_p \cdot \cos TS_c \cdot ZP + X_p \tag{24}$$

Therefore, the pathlength difference is given in terms of ϕ and H for points in this panel as

$$DP = (DZ + H + \phi \cdot T_c) \cdot S \tag{25}$$

VI. Computation of Shift Parameters

The sum of the weighted squared pathlength differences, $(DP)_p^2$, for all points at R_p in Fig. 4 is (see Eqs. 12–14, 18, 24, 25)

$$(DP)_p^2 = W_p \sum_{c=1}^{J_k} \frac{1}{J_k} S_p^2 \cdot (DZ_p + H + \phi \cdot T_c)^2 \tag{26}$$

where the subscript "p" on the right-hand side is appended to indicate terms depending on R_p and not on the summation parameter "c." By defining

$$T_p = \frac{1}{J_k} \sum_{c=1}^{J_k} T_c \tag{27}$$

$$T2_p = \frac{1}{J_k} \sum_{c=1}^{J_k} T_c^2 \tag{28}$$

Eq. (26) becomes, upon expanding,

$$(DP)_p^2 = W_p \cdot S_p^2 \cdot (DZ_p^2 + H^2 + \phi^2 \cdot T2_p + 2DZ_p \cdot H + 2H \cdot \phi \cdot T_p + 2DZ_p \cdot \phi \cdot T_p) \tag{29}$$

The weighted sum of the squared differences for all $(J_k \cdot n_k)$ points in this kth panel is

$$SS = \sum_{p=1}^{n_k} (DP)_p^2 \tag{30}$$

Taking the partial derivatives of SS with respect to H and ϕ leads to the following normal equations, which can be solved for the shift parameters that minimize Eq. (30) for this panel:

$$\begin{bmatrix} A & B \\ B & C \end{bmatrix} \begin{pmatrix} H \\ \phi \end{pmatrix} = \begin{pmatrix} D \\ E \end{pmatrix} \tag{31}$$

in which

$$A = \Sigma\, W_p \cdot S_p^2 \tag{32}$$

$$B = \Sigma\, W_p \cdot S_p^2 \cdot T_p \tag{33}$$

$$C = \Sigma\, W_p \cdot S_p^2 \cdot T_p^2 \tag{34}$$

$$D = -\Sigma\, W_p \cdot S_p^2 \cdot DZ_p \tag{35}$$

$$E = -\Sigma\, W_p \cdot S_p^2 \cdot DZ_p \cdot T_p \tag{36}$$

and the summations in Eqs. (32–36) are taken over the n_k radii defined for this panel.

Once H and ϕ are determined from Eq. (31), Eqs. (26) and (30) are used to obtain the weighted sum of squared differences. The minimized rms difference in half pathlength is then obtained from

$$\text{rms} = \tfrac{1}{2}(SS/n_k)^{1/2} \tag{37}$$

VII. Non-optimum End-Match Shift Parameters

For comparison, it is informative to perform a relatively simple computation to determine the difference in pathlength for a corner-match, non-minimum rms shift of the panel. In this case, the corners b, c, d, e of the parabolic panel are brought to the shaped surface without considering distances from the interior panel points to the shaped surface. To determine the corresponding values of H and ϕ, the sum $DZ + DELZ$ is set equal to zero for the panel corners. Therefore, in Eq. (24), let

$$T_A = V_A \cdot \cos(TR/2) \cdot R_A/2f \tag{38}$$

$$T_B = V_B \cdot \cos(TR/2) \cdot R_B/2f + (R_B - R_A) \cdot \cos(TR/2) \tag{39}$$

where

$$V_A = R_A^2\,[1 - \cos^2(TR/2)]/4f \tag{40}$$

$$V_B = R_B^2\,[1 - \cos^2(TR/2)]/4f \tag{41}$$

Consequently, the non-optimum shift parameters can be found from (see Eq. 23)

$$\begin{bmatrix} 1 & T_A \\ 1 & T_B \end{bmatrix} \begin{pmatrix} H \\ \phi \end{pmatrix} = \begin{pmatrix} DZA \\ DZB \end{pmatrix} \tag{42}$$

where DZA and DZB are the central focal-axis coordinate distances from the shaped to the parabolic panel surfaces.

In practice, the foregoing equations are adjusted to reflect the first and last radii defined for the panel by the DAR program, because it is unlikely that shaped surface coordinates will be supplied exactly at R_A and R_B.

VIII. Computer Program and Results

A computer program has been written to perform the calculations described. Input to the program consists of the focal length of the parabolic surface, the number of panel rings, the central sector angle of the innermost panel, the boundary radii for each panel ring, the number of panels in each ring that fit into the central sector, and the punched card output from the DAR program giving radius, focal-axis coordinate, and β angle.

Output from the program is sequential, beginning with the innermost panel rings and proceeding to the rim. For each panel, the output consists of the rms half-pathlength difference before and after shifting, coordinates, the shift parameters, original and new pathlength differences for points along the panel edges and centerline, and a summary designed to expedite field resetting of the panel that contains focal-axis and radial shift dimensions for panel corners. After all panel rings are processed, summary data for panel edges at R_A and R_B are combined in a single table. This table makes it convenient to determine focal and radial coordinate gaps and approaches between adjacent panel edges, which are not constrained during the fitting procedure. The current experience is that these gaps tend to be small; for the 64-m antenna, the maximum gap in the focal direction is about 1.5 mm, and the maximum approach in the radial direction is about 3 mm. The average gaps and approaches are considerably less. The radial approaches can either be contained within existing clearance spaces between adjacent panels or be accommodated by minor field trimming.

Both before and after fitting, the inner panel rings exhibit generally smaller pathlength differences than the outer rings. Therefore, if an extremely close fit to the shaped surface is required, it could be advisable to replace some of the outer panel rings with new panels contoured to the shaped surface. Consequently, a final tabulation that is output is the weighted half-pathlength differences for the reflector surface, considering the alternatives of retaining $1, 2, \cdots, m$ existing panel rings and providing $m-1, m-2, \cdots, 0$ new rings.

Table 1 shows a summary of the rms differences for each panel ring for the Mars DSS (DSS 14) 64-m antenna ($m = 9$) and the Venus DSS (DSS 13) 26-m antenna ($m = 7$) before and after fitting. Table 2 contains a summary of the reflector rms differences for various alternatives of retaining existing and supplying new panel rings. Data from Table 2 are plotted in Figs. 5 and 6. In Fig. 5, the broken line is for the alternative of reworking the last panel ring for the DSS 14 antenna by subdividing the existing ring into two rings with independent shift parameters. Figs. 5 and 6 show that, for either of these antennas, the rms differences resulting from best-fit rms shifts of the existing panels are small; therefore, it is appropriate to re-use most or all of the existing panels. The figures also show that the non-optimum corner match fit results in about double the foregoing differences.

References

1. Ludwig, A. C., "Antennas for Space Communications: 1. Shaped Reflector Cassegrain Antennas," in *Supporting Research and Advanced Development*, Space Programs Summary 37-35, Vol. IV, pp. 266–268. Jet Propulsion Laboratory, Pasadena, Calif., Oct. 31, 1965.
2. Jarvie, P., and Gerritson, R., *Dual Reflector Antenna System Design Program*, Document TR-66-700-13-2, Oct. 12, 1966 (JPL internal document).

Table 1. Individual panel ring differences

Panel numbers (in order of increasing radius)	Half-pathlength rms, mm					
	DSS 14 64-m antenna			DSS 13 26-m antenna		
	Before fit	rms fit	Corner fit	Before fit	rms fit	Corner fit
1	0.93	0.10	0.32	0.35	0.13	0.44
2	0.49	0.04	0.09	2.55	0.05	0.10
3	2.55	0.07	0.14	5.43	0.03	0.06
4	7.15	0.03	0.08	7.13	0.05	0.09
5	11.71	0.01	0.02	7.17	0.09	0.20
6	15.60	0.07	0.16	4.83	0.19	0.41
7	17.86	0.15	0.31	2.84	0.37	0.91
8	15.10	0.49	1.18	—	—	—
9	7.17	1.41	3.59	—	—	—

Table 2. Alternatives for retained parabolic vs new panel rings

Combined reflector half-pathlength rms differences, mm							
DSS 14 64-m antenna				DSS 13 26-m antenna			
Panel rings		rms fit	Corner fit	Panel rings		rms fit	Corner fit
Retained	New			Retained	New		
1	8	0.01	0.03	1	6	0.03	0.10
2	7	0.01	0.03	2	5	0.04	0.11
3	6	0.02	0.05	3	4	0.04	0.11
4	5	0.02	0.05	4	3	0.04	0.12
5	4	0.02	0.05	5	2	0.06	0.15
6	3	0.04	0.08	6	1	0.10	0.23
7	2	0.07	0.15	7	0	0.17	0.41
8	1	0.24	0.57	—	—	—	—
9	0	0.69	1.73	—	—	—	—

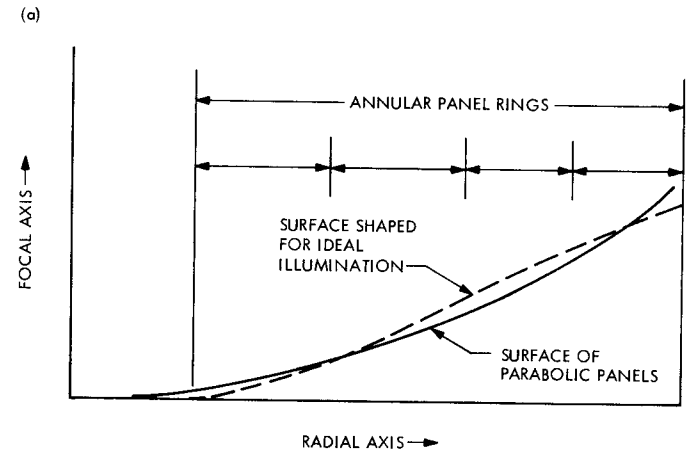

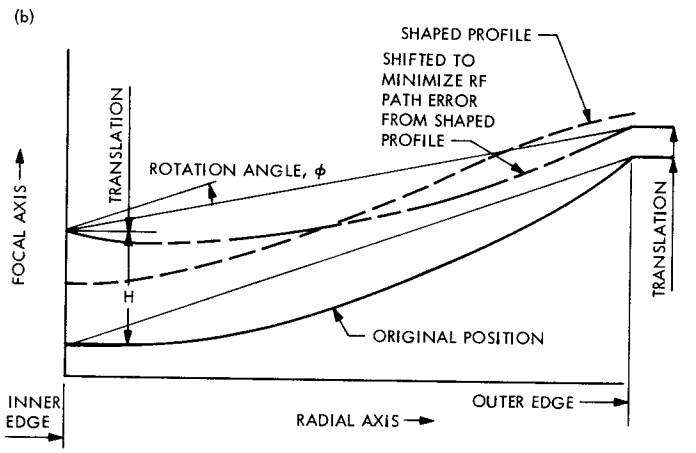

Fig. 1. Parabolic panels for shaped-surface reflector: (a) profile view of shaped vs parabolic surfaces, (b) resetting of typical parabolic panel

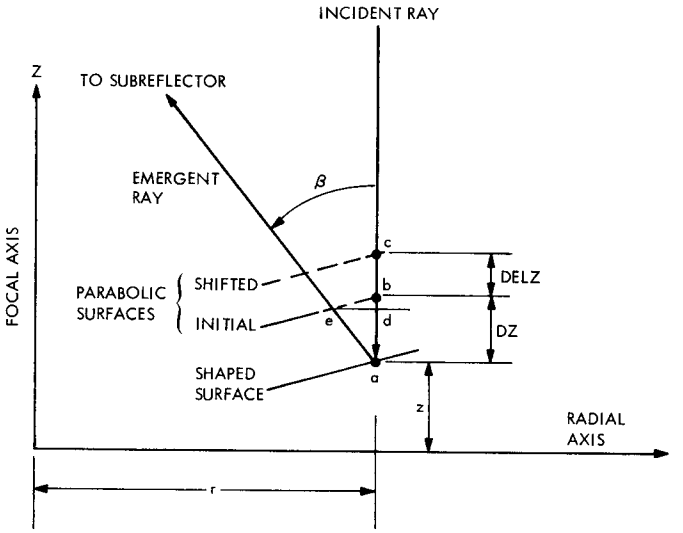

Fig. 2. Pathlength geometry

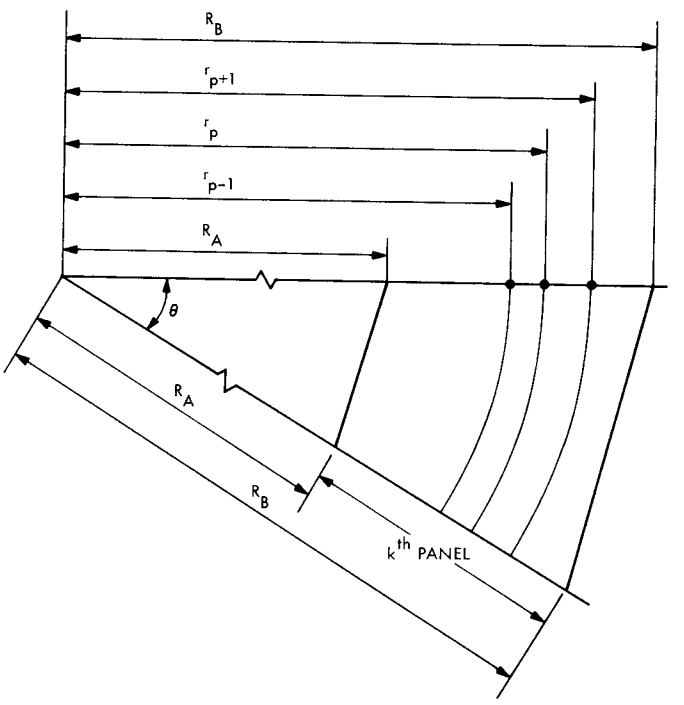

Fig. 3. Weighting factor geometry

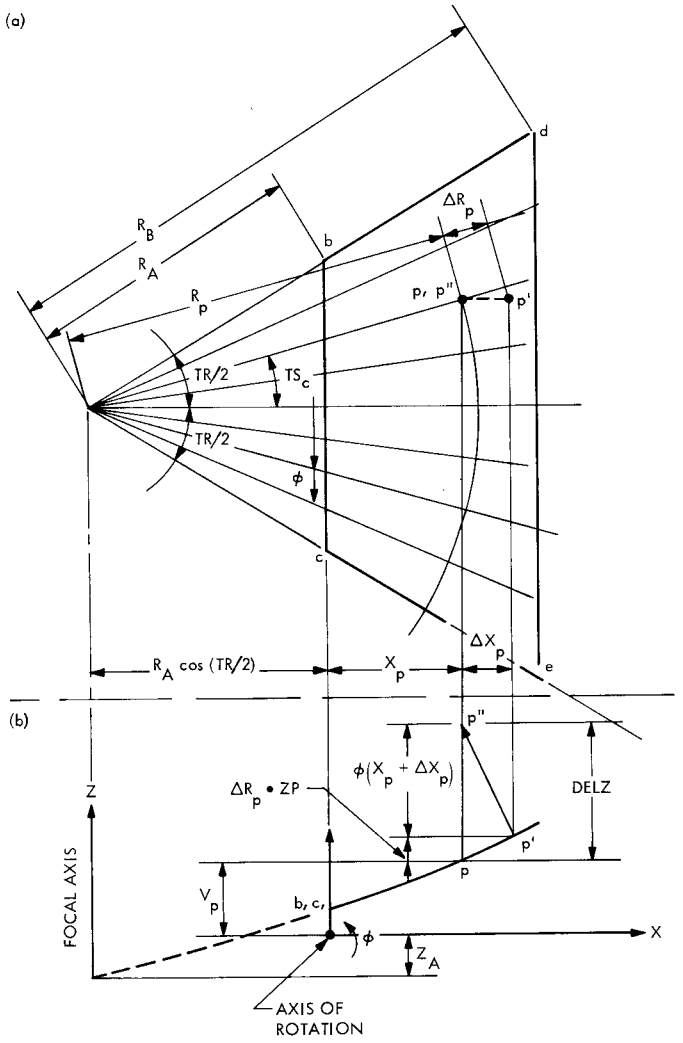

Fig. 4. Focal-axis coordinate shift for panel rotation: (a) panel projection on aperture plane, (b) side view of panel

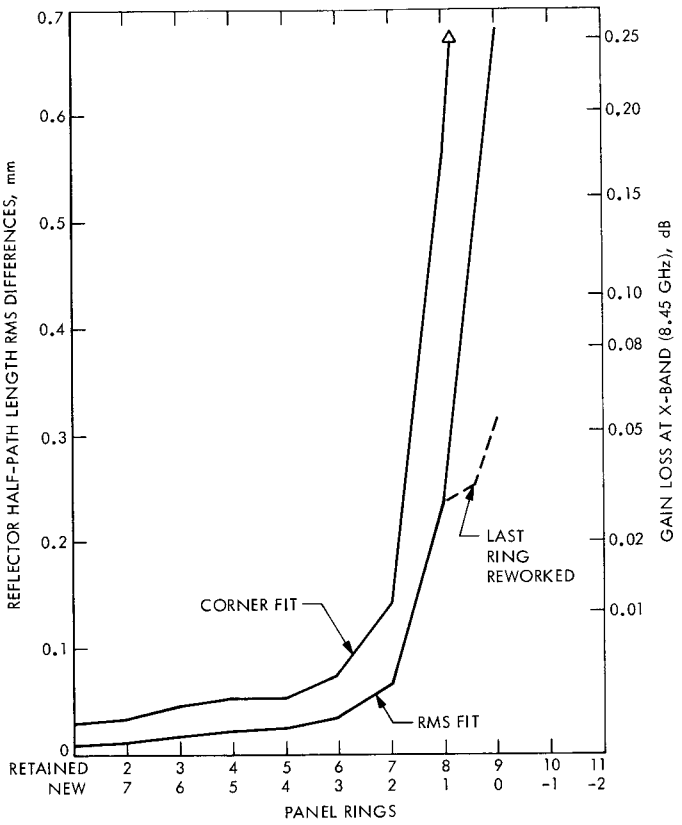

Fig. 5. Alternatives for retained vs new panel rings: DSS 14 antenna

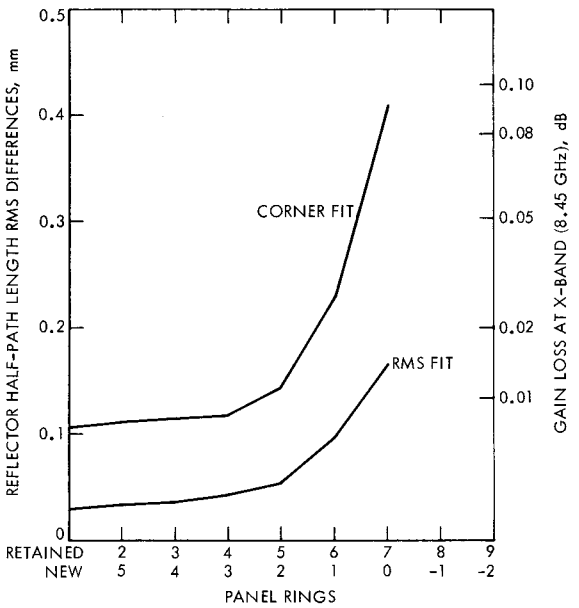

Fig. 6. Alternatives for retained vs new panel rings: DSS 13 antenna